**Chula Med J. July - August 2025;69(4):** 209 - 225 **DOI : 10.56808/2673-060X.**5598

**Original article**

# Dual role of Triphala extracts in breast cancer therapy: Enhanced paclitaxel cytotoxicity by ethanolic extract and cytoprotection by aqueous extract

**Supamas Charucharana[a, b], Poonlarp Cheepsunthorn[c], Chalisa Louicharoen Cheepsunthorn[d, *]**

[a] *Medical Sciences Program, Faculty of Medicine, Chulalongkorn University, Bangkok, Thailand*
[b] *Department of Applied Thai Traditional Medicine, Faculty of Sciences and Technology, Phranakhon Rajabhat University, Bangkok, Thailand*
[c] *Department of Anatomy, Faculty of Medicine, Chulalongkorn University, Bangkok, Thailand*
[d] *Department of Biochemistry, Faculty of Medicine, Chulalongkorn University, Bangkok, Thailand*

## Abstract

**Background:** Combining antioxidants with chemotherapy is an emerging strategy for reducing chemotoxicity in normal cells. Triphala (TPL), a polyphenol-rich Thai herbal formulation, has exhibited potential in enhancing chemotherapy efficacy; however, its interaction with paclitaxel in breast cancer treatment remains underexplored.
**Objective:** This study aimed to evaluate the effects of aqueous (TPL-w) and ethanolic (TPL-a) TPL extracts in combination with low-dose paclitaxel on breast cancer and non-tumorigenic mammary epithelial cells.
**Methods:** The bioactive components of TPL-w and TPL-a were identified using high-performance liquid chromatography. Thiazolyl blue tetrazolium bromide (MTT) and chloromethyl 22' ,72' - dichlorodihydrofluorescein diacetate (CM-$H_2$DCFDA) assays were employed to assess cell viability and reactive oxygen species (ROS) levels, respectively, in breast cancer (MDA-MB-231, MCF-7) and epithelial (MCF-10A) cells. Combination index values were calculated using CompuSyn, whereas quantitative polymerase chain reaction was used to analyze apoptosis- and antioxidant-related gene expressions.
**Results:** Gallic acid was the predominant compound identified in both extracts, with higher levels detected in TPL-a. Paclitaxel and TPL-a cotreatment exhibited greater cytotoxicity in breast cancer cells, particularly in MDA-MB-231, compared with that of TPL-w cotreatment, primarily through enhanced ROS accumulation and an elevated *BAX/BCL2* ratio, which led to apoptosis. TPL-a significantly downregulated superoxide dismutase (*SOD1)* and glutathione peroxidase (*GPX1)* expression in cancer cells, thereby enhancing oxidative stress. Conversely, TPL-w exhibited moderate cytotoxicity but effectively protected MCF-10A cells by upregulating the expression of *SOD1* and *GPX1*, reducing ROS levels, and lowering the *BAX/BCL2* ratio, thus enhancing cell survival.
**Conclusion:** TPL-a exhibited superior anticancer activity when combined with paclitaxel, whereas TPL-w provided stronger cytoprotection in normal cells. These findings highlight TPL-a's potential as a complementary chemotherapeutic agent and TPL-w's protective role, thereby warranting further investigation into their clinical applications.

**Keywords:** Antioxidant therapy, breast cancer, chemotherapy, gallic acid, paclitaxel, reactive oxygen species, synergistic effect, triphala.

Breast cancer is the most frequently diagnosed cancer and the second leading cause of cancer-related death among women. [1] It is classified according to its molecular markers, including estrogen receptor (ER), progesterone receptor (PR), and human epidermal growth factor receptor 2 (HER2). Among its subtypes, triple-negative breast cancer (TNBC), characterized by the absence of these three markers, is particularly aggressive and associated with a poor prognosis because of its high metastatic potential and limited options for targeted treatment. [2] Despite advancements in breast cancer therapy, TNBC

***Correspondence to: Chalisa Louicharoen Cheepsunthorn,** Department of Biochemistry, Faculty of Medicine, Chulalongkorn University, Bangkok 10330, Thailand.
E-mail: Chalisa.l@chula.ac.th
Received: October 10, 2024
Revised: May 22, 2025
Accepted: June 13, 2025

remains a major clinical challenge, necessitating the identification of novel therapeutic strategies.

A crucial aspect of cancer cell survival and proliferation is the regulation of redox homeostasis. [3] While normal cells maintain low levels of reactive oxygen species (ROS) for physiological functions, cancer cells generate elevated ROS levels, which are driven by heightened metabolic and mitochondrial activity. This oxidative stress can promote cancer progression by activating oncogenic pathways, although excessive ROS accumulation may also lead to oxidative damage and induce cell death. [4, 5] Recent studies have shown that ROS levels are consistently higher in cancer cells than in normal cells. [6] For instance, a recent study on breast cancer demonstrated that TNBC cells exhibited the highest basal levels of ROS, followed by ER-positive breast cancer cells, while non-tumorigenic cells exhibited the lowest ROS levels. This highlights a gradient that correlates with tumor aggressiveness and metabolic demand. [7]

This redox imbalance has been therapeutically exploited by chemotherapeutic agents such as paclitaxel (PX), a taxane-based drug that disrupts microtubule dynamics and halts mitosis. [8] In addition to its cytostatic action, PX increases the generation of intracellular ROS, forcing cancer cells beyond their oxidative stress threshold and promoting apoptosis. [9, 10] However, elevated ROS generation during treatment can also damage normal tissues, thereby contributing to dose-limiting toxicities. [11] Therefore, there is a growing interest in strategies that selectively modulate oxidative stress in cancer cells while preserving normal cell viability.

Recent attention has focused on the potential of antioxidant cotreatment in cancer therapy. Triphala (TPL), a traditional herbal formulation composed of *Terminalia chebula (T. chebula)*, *Terminalia bellerica (T. bellerica)*, and *Phyllanthus emblica (P. emblica),* is commonly prepared via aqueous (TPL-w) or ethanolic (TPL-a) extraction, resulting in distinct phytochemical profiles. TPL-w is rich in water-soluble compounds, such as gallic acid, ellagic acid, and vitamin C, and exhibits strong antioxidant properties, while TPL-a contains higher levels of polyphenols, flavonoids, and tannins and demonstrates potent pro-apoptotic and cytotoxic effects against cancer cells. [7, 12] Previous studies have shown that TPL-w and TPL-a inhibit proliferation, induce apoptosis, and suppress tumor growth in breast cancer cell lines, including ER-positive (MCF-7), PR-positive (T47D), and TNBC (MDA-MB-231), without exhibiting cytotoxic effects on normal breast epithelial cells or peripheral blood mononuclear cells. [13-15] In addition, TPL-w has demonstrated protective effects against oxidative damage in animal models. [16] Although both TPL extracts have demonstrated anticancer activity, comparative studies on their ability to selectively protect normal cells from chemotherapy-induced oxidative stress while enhancing anticancer efficacy remain limited. Furthermore, it is unclear whether differences in bioactive compound levels between TPL-w and TPL-a affect the modulation of redox balance in cancer against normal cells.

This study aimed to evaluate the protective effects of TPL-w and TPL-an on human breast epithelial cells (MCF-10A) against PX-induced cytotoxicity. In addition, this study investigated whether the combination of TPL extracts with PX enhanced the anticancer activity in MDA-MB-231 and MCF-7 cell lines by modulating the antioxidant responses and maintaining the redox balance. The findings of this study may contribute to the development of combination therapies that improve chemotherapy outcomes while minimizing damage to healthy cells.

## Materials and methods

The study protocol was reviewed and approved by the Institute Ethics Committee of the Faculty of Medicine, Chulalongkorn University, Bangkok, Thailand (IRB no. 511/64).

### *TPL extraction*

Dried powders of *T. chebula*, *T. bellerica*, and *P. emblica* were obtained from Vejpong Pharmacy Co., Ltd. (Bangkok, Thailand). TPL-a was prepared as previously described. [7] TPL-w was prepared using the modified protocol described by Naik GH, *et al.* [17] In brief, 75 g of TPL powder was dissolved in 250 mL of distilled water, heated at 90°C for 30 min, cooled to room temperature, and centrifuged to remove the debris. The supernatant was filtered through 11-µm Whatman filter paper and lyophilized. The lyophilized TPL-w was stored at 20°C under light-protected conditions. For experiments, a stock solution of 10 mg/mL was prepared by dissolving the dried extract in 5.0% dimethyl sulfoxide (DMSO) (D2660, Sigma-Aldrich, MO, USA). Working solutions were prepared by diluting the stock solution in the cell culture medium and filtered using a 0.2-µm syringe filter (Johnson Test Papers Ltd., Oldbury, UK) before use.

### *PX preparation*

PX (Sigma-Aldrich) was dissolved in DMSO to a final concentration of 10 mM and stored at −20°C under light-protected conditions. Before use, PX was diluted in the cell culture medium, ensuring that the final DMSO concentration remained below 0.1% to prevent DMSO-induced cytotoxicity. All working dilutions were freshly prepared immediately before use.

### *Free radical scavenging activity*

The antioxidant activity of the TPL extracts was evaluated using the 2,2-diphenyl-1-picrylhydrazyl (DPPH) radical scavenging assay, as previously described. [18] In brief, 100 µL of 0.2 mM DPPH solution (MilliporeSigma, USA) in methanol was mixed with 100 µL of TPL extract at varying concentrations (10–500 µg/mL). The mixture was vortexed and incubated in the dark at 37°C for 30 min. In methanol, DPPH appears violet and fades to yellow upon reduction by antioxidants. Absorbance was measured at 515 nm using a microplate reader (Biotek Synergy HT, USA). Gallic acid served as the positive control, whereas the control sample contained no extract. The DPPH radical scavenging activity percentage was calculated using the following formula:

$$\text{DPPH scavenging activity (\%)} = (A_0 - A_1) / A_0 \times 100$$

where $A_0$ represents the absorbance of the control and $A_1$ represents the absorbance of the sample.

### *High-performance liquid chromatography (HPLC) quantification*

The TPL extracts were characterized using HPLC with an Agilent 1260 series system equipped with a photodiode array detector and autosampler. The separation conditions were modified based on previous studies. [19] Chromatographic separation was performed using a Poroshell 120 EC-C18 column (2.7 µm, 4.6 × 150 mm) maintained at 26°C. The mobile phase consisted of 0.1% acetic acid (solvent A) and acetonitrile (solvent B) delivered at a flow rate of 1 mL/min. The injection volume was 20 µL, and detection was performed at 270 nm. Gallic acid was used as the standard control. Identification of gallic acid content in the TPL extract was determined by comparing the retention times and absorption spectra of the corresponding peaks with those of the gallic acid standard. TPL samples (50 µg/mL) and gallic acid standards (25–100 µg/mL) were analyzed in triplicate. Data were processed using Agilent ChemStation software (Agilent, USA).

### *Determination of phenolic and flavonoid contents*

The total phenolic content in the TPL extracts was determined using the Folin–Ciocalteu colorimetric method, as previously described. [20] Briefly, 1 mg/mL of the TPL extracts were mixed with 0.2 M Folin–Ciocalteu reagent and incubated for 5 min. Subsequently, 8.0% sodium carbonate solution was added, and the mixture was incubated for 60 min in the dark. The resulting dark blue color, indicative of phenol oxidation, was measured at 756 nm using a microplate reader. All experiments were performed in triplicate. Phenolic content was calculated from a gallic acid standard curve and expressed as mg of gallic acid equivalents per g of sample (mg GAE/g).

Total flavonoid content was measured using a previously described colorimetric assay method with slight modifications. [21] In a 1.5 mL test tube, 50 µL of TPL extract (1 mg/mL) was mixed with 320 µL of distilled water, followed by the addition of 15 µL of 5.0% sodium nitrite and 15 µL of 10.0% aluminum chloride. After incubation, 0.1 mL of 1 M sodium hydroxide was added. Absorbance was measured at 510 nm against a blank reagent using a microplate reader. Catechin served as the standard for the calibration curve, and flavonoid content was expressed as mg of catechin equivalents per g of sample dry weight (mg CE/g).

### *Cell culture*

The human breast cancer cell lines MDA-MB-231 (ATCC no. HTB-26) and MCF-7 (ATCC no. HTB-22) were obtained from the American Type Culture Collection (ATCC, USA). Both cell types were cultured in Dulbecco's Modified Eagle Medium (DMEM; HyClone, USA) supplemented with 5.0% heat-inactivated fetal bovine serum; Gibco, MA, USA), 100 U/mL penicillin/streptomycin, and 100 U/mL HEPES (Gibco).

Human normal mammary epithelial cells (MCF-10A, ATCC no. CRL-10317) were cultured in DMEM/F12 (HyClone) supplemented with 20 ng/mL epidermal growth factor (PeproTech, NJ, USA), 100 ng/mL cholera toxin, 10 µg/mL insulin, 500 ng/mL hydrocortisone (all from Sigma-Aldrich), and 5.0% horse serum (Gibco).

All cell lines were maintained at 37°C under 5.0% $CO_2$, conditions in a 95.0% humidified incubator (BINDER, Tuttlingen, Germany). We passaged cells twice weekly using 0.25% trypsin with 0.02% EDTA. Cells between passages 5 and 20 were used in the experiments. All procedures were performed under aseptic conditions following standard cell culture protocols.

### *Cytotoxicity and combination index determination*

To determine the optimal concentrations of TPL and PX, cells were seeded in 96-well plates (Corning, NY, USA) at a density of $4\times10^4$ cells/well and incubated for 24 h. Cells were treated with varying concentrations of TPL (25–2000 µg/mL) and PX (0.1–2 µM) for 48 h to calculate the $IC_{50}$ values. Cell viability was assessed using the thiazolyl blue tetrazolium bromide (MTT) assay (M5655, Sigma-Aldrich). After treatment, cells were incubated with 2 mg/mL MTT for 4 h at 37°C. The resulting formazan crystals were dissolved in DMSO, and the optical density was measured at 570 nm. Cell viability was calculated using the following formula:

$$\text{Cell viability (\%)} = (OD_{treatment} / OD_{control}) \times 100$$

For combination studies, non-toxic concentrations of TPL (50–200 µg/mL) were combined with PX (0.5 µM), and the combination index (CI) was calculated using the Chou-Talalay method via the CompuSyn software.

$$CI = [(D)_1/(Dx)_1] + [(D)_2/(Dx)_2]$$

Where $(D)_1$ and $(D)_2$ represent the concentrations of TPL and PX used together to achieve 50.0% of the drug effect, and $(Dx)_1$ and $(Dx)_2$ are the concentrations of TPL and PX, respectively, when used individually to achieve the same effect. The CI values were interpreted as follows: CI < 1 indicated synergism, CI = 1 indicated an additive effect, and CI > 1 indicated antagonism. [22]

### *Measurement of intracellular ROS*

Intracellular ROS levels were quantified using chloromethyl 22 ,72 -dichlorodihydrofluorescein diacetate (CM-$H_2$DCFDA) (Invitrogen, MA, USA). Cells were seeded in black, clear-bottom 96-well plates (Corning) at a density of $4\times10^4$ cells/well, treated as indicated, and incubated with Hanks' Balanced Salt Solution (HBSS) (Gibco) containing 10 µM CM-$H_2$DCFDA for 30 min at 37°C. Following incubation, the solution was removed, and cells were washed and incubated in HBSS under dark conditions for an additional 6 h at 37°C. The fluorescence intensity was measured using a microplate reader at an excitation wavelength of 495 nm and an emission wavelength of 525 nm. The ROS levels were normalized to cell viability and expressed relative to the untreated controls.

### *Reverse transcriptase-quantitative polymerase chain reaction (RT-qPCR)*

Total RNA was extracted using Trizol reagent (Thermo Fisher Scientific, MA, USA), and cDNA was synthesized using the RevertAid First Strand cDNA Synthesis Kit (Thermo Fisher Scientific), according to the manufacturer's instructions. Gene expression was quantified using SYBR Green-based qPCR with previously described primers. [7] Each qPCR reaction contained 5 µL of 2X Maxima SYBR Green Master Mix, 2 µL of nuclease-free water, 2 µM each of forward and reverse primers, and cDNA template, for a final volume of 10 µL. Amplification was performed using a thermocycler (Thermo Fisher Scientific) under the following conditions: initial denaturation at 95°C for 15 min, followed by 40 cycles of 95°C for 15 sec, primer-specific annealing temperatures for 30 sec, and 72°C for 30 sec. Gene expression levels were normalized to that of β-actin as an internal control and analyzed using the $2^{-\Delta\Delta Ct}$ method.

### *Statistical analysis*

Data was analyzed using SPSS version 29.0 (IBM Corp., NY, USA). All experiments were performed in triplicate (n = 3), and results are presented as the mean ± standard error of the mean (SEM). Statistical significance was determined using one-way analysis of variance, followed by Tukey's post hoc test for multiple comparisons. $P < 0.05$ was considered statistically significant.

## Results

### *Free radical scavenging activity*

The antioxidant properties of the TPL extract were evaluated using the DPPH assay, and the TPL-w and TPL-a extracts were compared with gallic acid as the standard (**Figure 1A**). The free radical scavenging activity increased in a concentration-dependent manner for both the extracts and gallic acid. The highest tested concentrations were 300 µg/mL for TPL-w, 200 µg/mL for TPL-a, and 75 µg/mL for gallic acid. At these concentrations, the maximum DPPH radical scavenging activities were 91.9 ± 0.8% for TPL-w, 92.7 ± 0.3% for TPL-a, and 94.3 ± 1.1% for gallic acid.

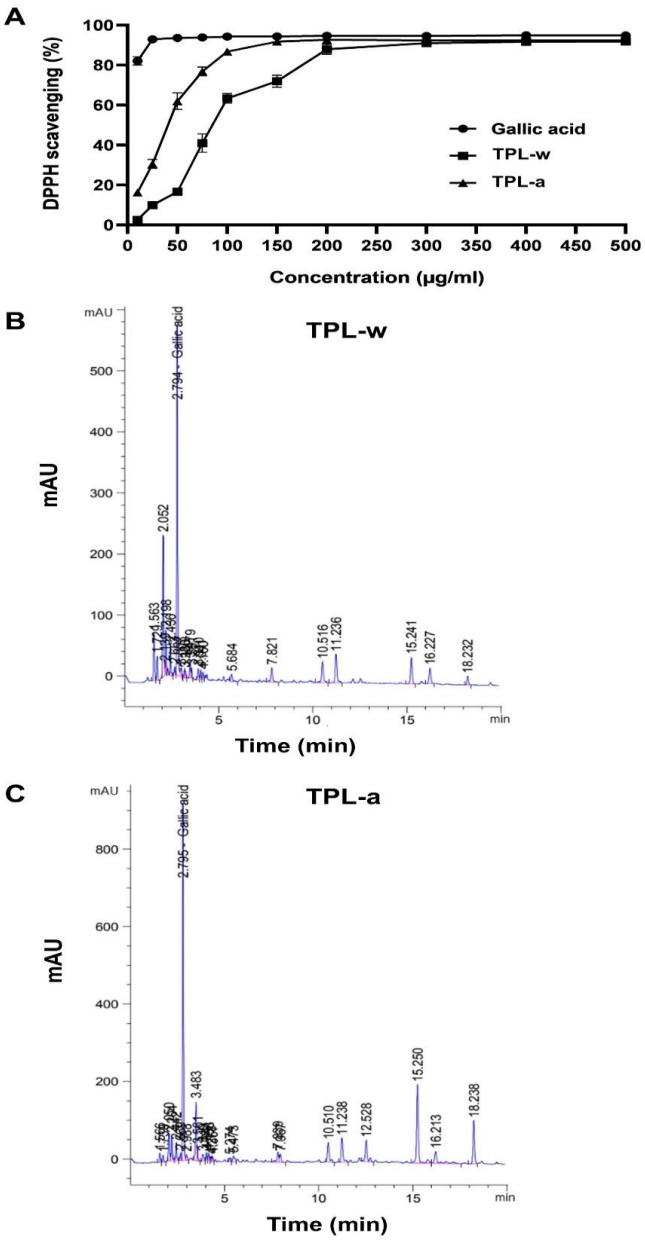


**Figure 1.** DPPH free radical scavenging activity of TPL extract compared to gallic acid (**A**); HPLC chromatograms of TPL-w (**B**); and TPL-a (**C**). Data are presented as mean ± SEM from at least three independent experiments, each performed in triplicate.

### *Total phenolic and flavonoid contents*

The antioxidant properties of the TPL extract were further evaluated by quantifying its total phenolic and flavonoid content. The total phenolic content was expressed as mg GAE/g, whereas the total flavonoid content was expressed as mg CE/g. All measurements were performed in triplicate. As shown in **Table 1**, the phenolic contents of TPL-w and TPL-a were 376.0 ± 6.5 mg GAE/g and 583.0 ± 3.2 mg GAE/g, respectively. Similarly, the total flavonoid content was 100.6 ± 1.3 mg CE/g for TPL-w and 129.5 ± 0.7 mg CE/g for TPL-a.

### *HPLC quantification of the TPL extracts*

The bioactive compounds in the TPL extract were analyzed using HPLC. The chromatograms are presented in **Figure 1B** and **1C,** and the corresponding results are summarized in **Table 2**. TPL-w (**Figure 1B**) and TPL-a (**Figure 1C**) exhibited prominent peaks that corresponded to gallic acid, with retention times of 2.794 and 2.795 min, respectively. The gallic acid concentration was 83.7 ± 1.4 µg/mL in TPL-w and 129.1 ± 0.6µg/mL in TPL-a, thus highlighting gallic acid as the predominant phenolic compound in the TPL extracts.

**Table 1.** Total phenolic and flavonoid contents of TPL.

| Extract | Total phenolic (mg GAE/g) | Total flavonoids (mg CE/g) |
|---|---|---|
| TPL-w | 376.0 ± 6.5 | 100.6 ± 1.3 |
| TPL-a | 583.0 ± 3.2 | 129.5 ± 2.7 |

**Table 2.** HPLC analysis of TPL identifying gallic acid as the primary compound.

| Compound | Extract | Retention time (min) | Area (mAU*s) | Area (%) | Amount (µg/ml) |
|---|---|---|---|---|---|
| **Gallic acid** | TPL-w | 2.797 | 1,934.1 ± 22.5 | 35.2 ± 0.7 | 83.7 ± 1.4 |
| | TPL-a | 2.795 | 3,062.6 ± 10.8 | 33.3 ± 0.3 | 129.1 ± 0.6 |

### *Cytotoxicity of TPL and PX in breast cancer and epithelial cell lines*

To determine the optimal concentration for the subsequent combination experiments, MDA-MB-231, MCF-7, and MCF-10A cells were treated with various concentrations of PX, TPL-w, and TPL-a extracts for 48 h. All compounds reduced the cell viability in a concentration-dependent manner **(Figure 2). Table 3** summarizes the IC values ($IC_{10}$–$IC_{50}$) of PX, TPL-w, and TPL-a in the breast cancer cells and epithelial cell lines, thereby providing a basis for selecting the appropriate concentrations. Based on these results, TPL-w and TPL-a extracts at nontoxic concentrations ($IC_{10}$–$IC_{20}$) were selected for use in the combination experiments with 0.5 µM PX or its corresponding $IC_{30}$–$IC_{40}$ range.

### *Combination effect of TPL and PX on breast cancer cells and epithelial cell lines*

Low-dose PX significantly reduced cell viability in MDA-MB-231, MCF-7, and MCF-10A cells by 75.3%, 70.4%, and 44.1%, respectively ($P < 0.001$) (**Figure 3A, C, E**; **Figure 4A, C, E**). The combination of PX with either TPL-w (**Figure 3B, D; Table 4**) or TLP-a (**Figure 4B, D; Table 4**) further enhanced the cytotoxicity, thus demonstrating a synergistic effect. In MDA-MB-231 cells, the combination reduced cell viability by 36.6–45.3% ($P < 0.001$) with TPL-w and 30.1–45.6% ($P < 0.001$) with TPL-a. In MCF-7 cells, viability decreased by 32.3–44.5% ($P = 0.005$, $P < 0.001$) with TPL-w and by 29.1–45.7% ($P = 0.022$, $P < 0.001$) with TPL-a. Importantly, TPL alone did not affect the MCF-10A cell viability (**Figure 3E, 4E**). Moreover, the combination of TPL and PX increased MCF-10A cell viability, which suggests a potential protective effect on normal cells (**Figure 3F, Figure 4F**).

### *Combination effect of TPL and PX on ROS production in breast cancer cells and epithelial cell lines*

The impact of the combination treatment of PX with either TPL-w or TPL-a on the intracellular ROS levels was evaluated considering the elevated basal ROS levels in cancer cells. The ROS levels were normalized to cell viability. Low-dose PX significantly increased ROS levels in MDA-MB-231 (1.6-fold, $P < 0.001$), MCF-7 (1.5-fold, $P < 0.001$), and MCF-10A cells (1.7-fold, $P < 0.001$) compared with those of the controls (**Figure 5**). Combining TPL-w or TPL-a with PX further elevated the ROS levels in a concentration-dependent manner in the breast cancer cells (**Figure 5A-D**). In MDA-MB-231 cells, the ROS levels increased 1.3–1.4-fold with 100 and 200 µg/mL TPL-w ($P = 0.028$ and $P = 0.005$) (**Figure 5A**) and 1.3–1.5-fold with TPL-a ($P = 0.011$ and $P = 0.002$) (**Figure 5B**). Similarly, in MCF-7 cells, the ROS levels increased 1.2–1.3-fold with TPL-w ($P = 0.011$ and $P = 0.006$) (**Figure 5C**) and 1.4–1.5-fold with TPL-a ($P = 0.007$ and $P = 0.005$) (**Figure 5D**), thus demonstrating the synergistic effect of TPL and PX in enhancing ROS production in breast cancer cells.

In contrast, TPL did not increase the ROS levels in non-tumorigenic MCF-10A cells (**Figure 5E-F**). Instead, TPL significantly attenuated PX-induced ROS levels at 100 and 200 µg/mL, reducing them by 1.3–1.5-fold ($P = 0.005$ and $P < 0.001$) with TPL-w and 1.4–1.5-fold ($P = 0.003$ and $P < 0.001$) with TPL-a. This suggests that TPL has a protective effect against PX-induced oxidative stress in normal mammary epithelial cells. These findings highlight the dual role of TPL in enhancing ROS-mediated cytotoxicity in breast cancer cells and protecting normal cells from oxidative damage.

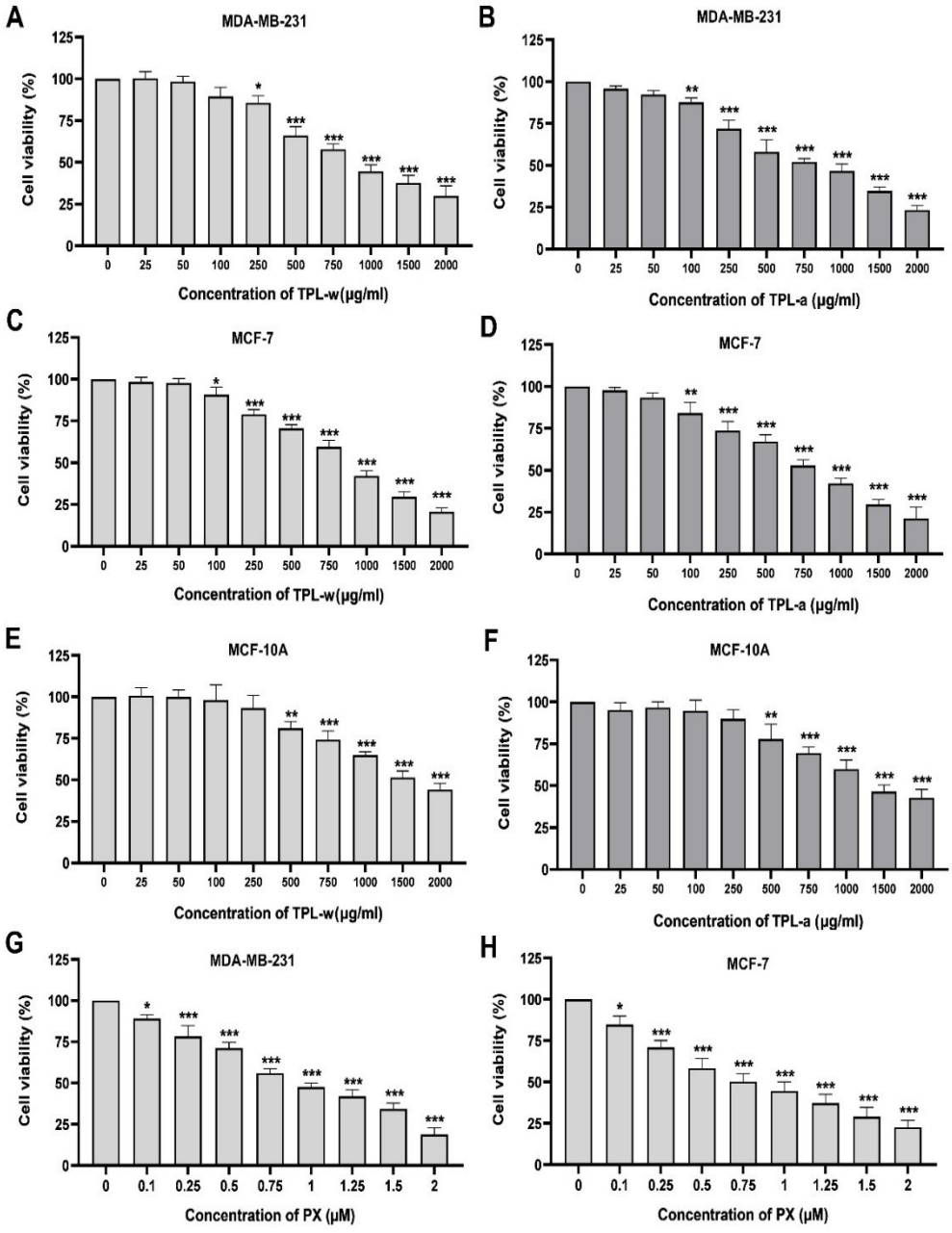


**Figure 2.** Effect of TPL-w (**A, C, E**) and TPL-a (**B, D, F**); as well as PX (**G, H**) on cell viability in MDA-MB-231 (**A, B, G**); MCF-7 (**C, D, H**); and MCF-10A (**E, F**) cells following 48 h of treatment. Data are presented as mean ± SEM from three independent experiments ($^{*}P < 0.05$; $^{**}P < 0.01$; $^{***}P < 0.001$ compared to untreated cells).

**Table 3.** IC values of PX, TPL-w, and TPL-a extracts in MDA-MB-231, MCF-7, and MCF-10A cell lines.

| Compound | IC value | MDA-MB-231 | MCF-7 | MCF-10A |
|---|---|---|---|---|
| **TPL-w (µg/ml)** | $IC_{10}$ | 113 | 102 | 295 |
| | $IC_{20}$ | 212 | 298 | 488 |
| | $IC_{30}$ | 454 | 470 | 736 |
| | $IC_{40}$ | 655 | 676 | 1184 |
| | $IC_{50}$ | 896 | 842 | 1434 |
| **TPL-a (µg/ml)** | $IC_{10}$ | 97 | 95 | 321 |
| | $IC_{20}$ | 202 | 189 | 605 |
| | $IC_{30}$ | 310 | 293 | 863 |
| | $IC_{40}$ | 545 | 506 | 1398 |
| | $IC_{50}$ | 723 | 702 | 1804 |
| **PX (µM)** | $IC_{10}$ | 0.1 | 0.1 | NA |
| | $IC_{20}$ | 0.2 | 0.1 | NA |
| | $IC_{30}$ | 0.5 | 0.3 | NA |
| | $IC_{40}$ | 0.7 | 0.5 | NA |
| | $IC_{50}$ | 0.8 | 0.6 | NA |

NA, not applicable.

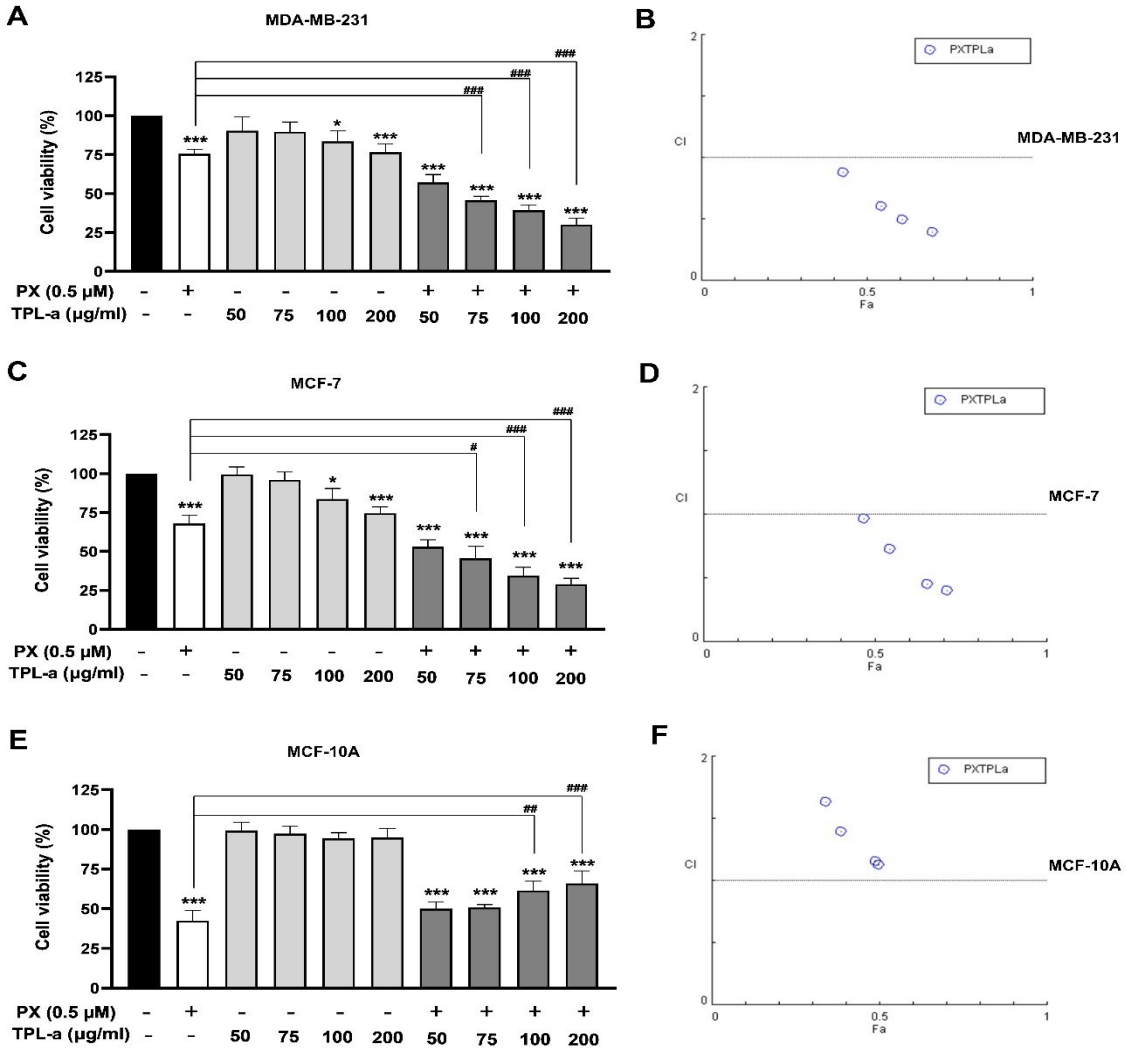


**Figure 3.** Combination effects of TPL-w and PX on cell viability in MDA-MB-231 **(A)**; MCF-7 **(C)**; and MCF-10A **(F)** cells; with corresponding CI plots **(B, D, F)**. Data are presented as mean ± SEM from three independent experiments. $^{*}P < 0.05$; $^{***}P < 0.001$ compared to untreated cells; $^{\#}P < 0.05$; $^{\#\#}P < 0.01$; $^{\#\#\#}P < 0.001$ compared to PX-treated cells.

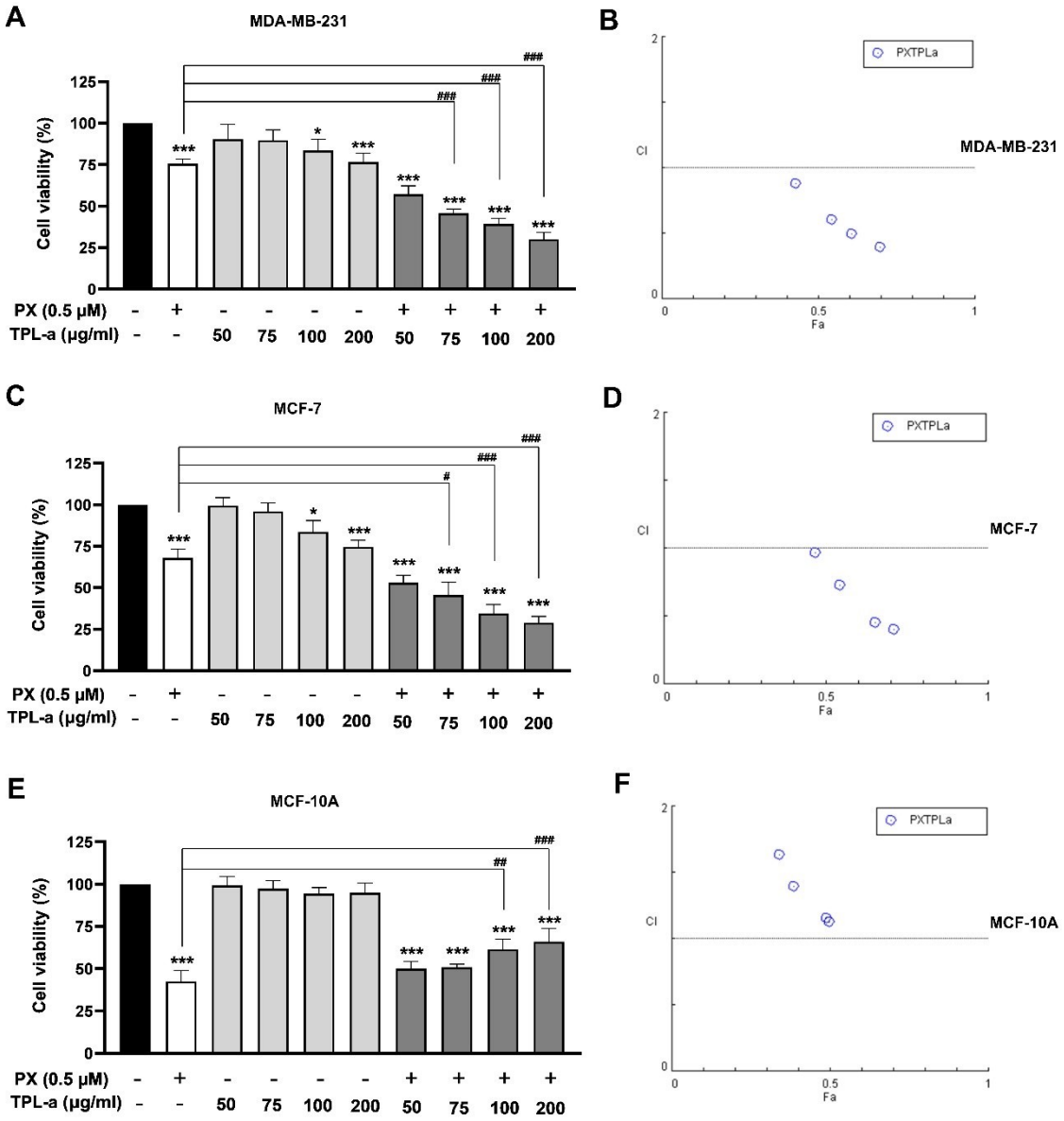


**Figure 4**. Combination effects of TPL-a and PX on cell viability in MDA-MB-231 **(A)**; MCF-7 **(C)**, and MCF-10A **(E)** cells; with corresponding CI plots **(B, D, F)**. Data are presented as mean ± SEM from three independent experiments. $^{*}P < 0.05$; $^{***}P < 0.001$ compared to untreated cells; $^{\#}P < 0.05$; $^{\#\#}P < 0.01$; $^{\#\#\#}P < 0.001$ compared to PX-treated cells.

**Table 4.** CI values of low-dose PX and TPL-w/TPL-a in MDA-MB-231, MCF-7, and MCF-10A cells. The interpretation of CI values was as follows: CI < 1 represented synergy, CI = 1 represented an additive effect, and CI > 1 represented antagonism.

| | 0.5 μM PX + TPL (μg/ml) | CI Value (MDA-MB-231) | CI Value (MCF-7) | CI Value (MCF-10A) |
|---|---|---|---|---|
| **TPL-w** | **50** | 0.97 | 1.40 | 1.19 |
| | **75** | 0.67 | 0.96 | 1.29 |
| | **100** | 0.61 | 0.70 | 1.43 |
| | **200** | 0.53 | 0.47 | 1.58 |
| **TPL-a** | **50** | 0.88 | 0.97 | 1.13 |
| | **75** | 0.60 | 0.73 | 1.16 |
| | **100** | 0.50 | 0.45 | 1.40 |
| | **200** | 0.39 | 0.40 | 1.64 |

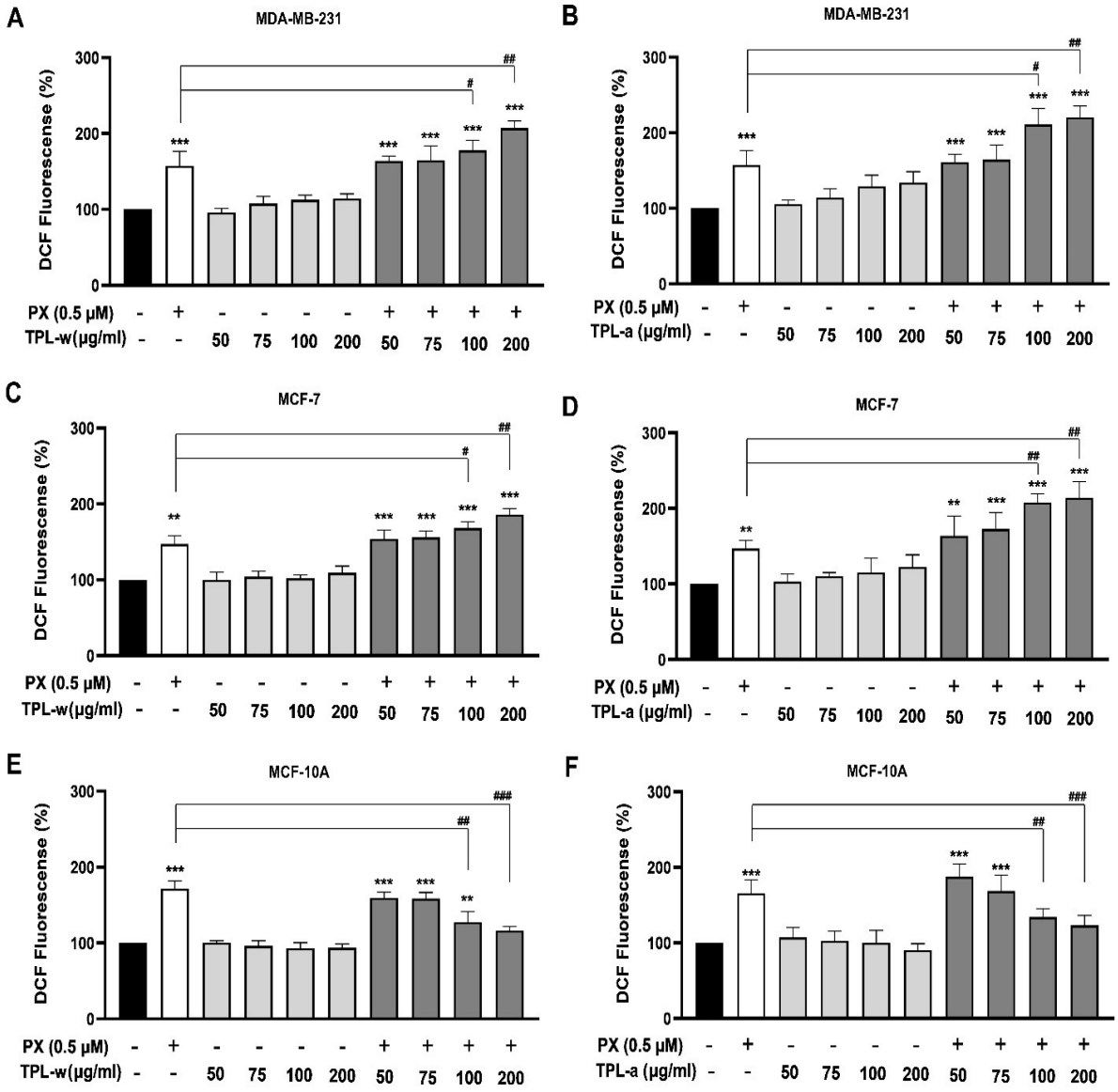


**Figure 5**. Effects of TPL-w (**A, C, E**) and TPL-a (**B, D, F**) combined with low-dose PX on intracellular ROS levels in MDA-MB-231 (**A, B**); MCF-7 (**C, D**), and MCF-10A (**E, F**). Data are represented as mean ± SEM from three independent experiments performed in triplicate. Statistical significance was defined as $^{*}P < 0.05$; $^{**}P < 0.01$; $^{***}P < 0.001$ compared to untreated cells; $^{\#}P < 0.05$; $^{\#\#}P < 0.01$; $^{\#\#\#}P < 0.001$ compared to PX-treated cells.

### *Combination effect of TPL and PX on apoptosis-related gene expression in breast cancer cells and epithelial cell lines*

The *BAX/BCL2* expression ratio was used to evaluate the induction of apoptosis. Low-dose PX significantly increased the *BAX/BCL2* ratio in MDA-MB-231 (5.9-fold, $P < 0.001$), MCF-7 (5.2-fold, $P = 0.002$), and MCF-10A (6.8-fold, $P < 0.001$) compared with those of untreated controls (**Figure 6**). In breast cancer cells, the combination of PX with 100 or 200 µg/mL of TPL extracts further elevated the *BAX/BCL2* ratio compared with that of PX alone, thus indicating enhanced apoptosis. In MDA-MB-231 cells, 200 µg/mL of TPL-w increased the ratio by 1.7-fold ($P = 0.009$), whereas 100 and 200 µg/mL of TPL-a caused a 2.2–2.4-fold increase ($P = 0.009$ and $P < 0.001$) (**Figure 6A, B**). Similarly, in MCF-7 cells, the ratio increased by 1.9-fold with 200 µg/mL of TPL-w ($P < 0.001$) and 2.2–2.4-fold with 100 and 200 µg/mL of TPL-a ($P = 0.002$ and $P < 0.001$) (**Figure 6C, D**), thereby demonstrating a synergistic apoptosis effect.

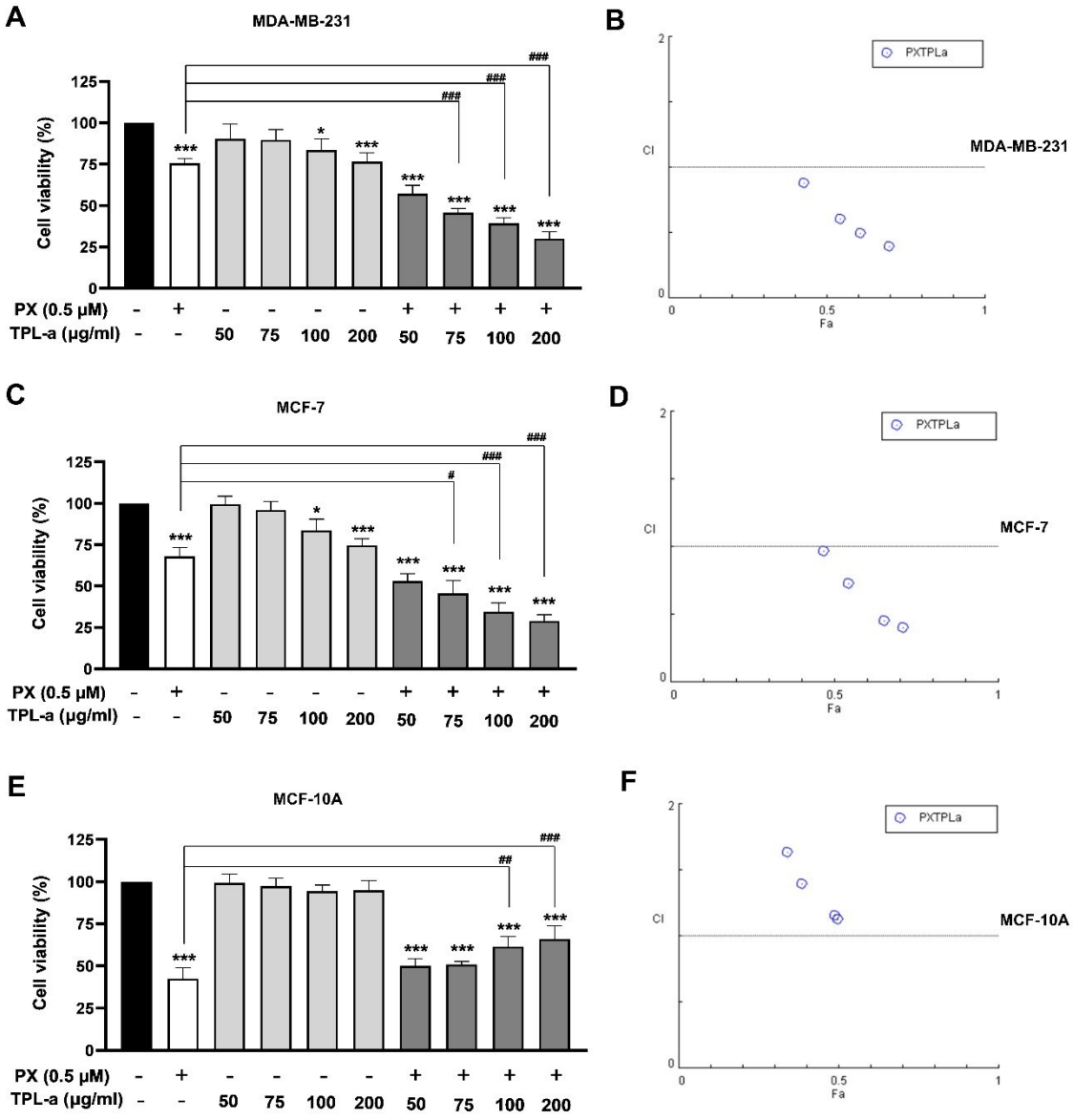


**Figure 6** Effects of TPL-w (**A, C, E**) and TPL-a (**B, D, F**), combined with low-dose PX, on the *BAX/BCL2* expression ratio in MDA-MB-231 (**A, B**), MCF-7 (**C, D**), and MCF-10A (**E, F**) cells. mRNA expression levels were normalized to β-actin. Data are represented as mean ± SEM from three independent experiments performed in triplicate. Statistical significance was defined as $^{*}P < 0.05$; $^{**}P < 0.01$; $^{***}P < 0.001$ compared to untreated cells, and $^{\#}P < 0.05$; $^{\#\#}P < 0.01$; $^{\#\#\#}P < 0.001$ compared to PX-treated cells.

In contrast, the combination treatment reduced the *BAX/BCL2* ratio in non-tumorigenic MCF-10A cells in a concentration-dependent manner. TPL at 100 and 200 μg/mL significantly lowered the ratio compared with that of PX alone, with a 1.9–2.4-fold decrease for TPL-w ($P = 0.011$ and $P < 0.001$) and a 2.3–3.0-fold reduction for TPL-a (both $P < 0.001$) (**Figure 6E, F**). These findings suggest that TPL enhances apoptosis in breast cancer cells and protects normal epithelial cells against PX-induced apoptosis.

### *Combination effect of TPL and PX on antioxidant-related gene expression in breast cancer cells and epithelial cell lines*

To assess the impact of PX and TPL on the redox balance regulation in breast cancer cells, the mRNA expression of key antioxidant enzymes, such as superoxide dismutase (*SOD1*), glutathione peroxidase (*GPX1*), and catalase (*CAT*), was analyzed. PX treatment alone significantly downregulated *SOD1* expression in the MDA-MB-231 (2.0-fold, $P = 0.045$), MCF-7 (2.1-fold, $P = 0.042$), and MCF-10A (4.5-fold,

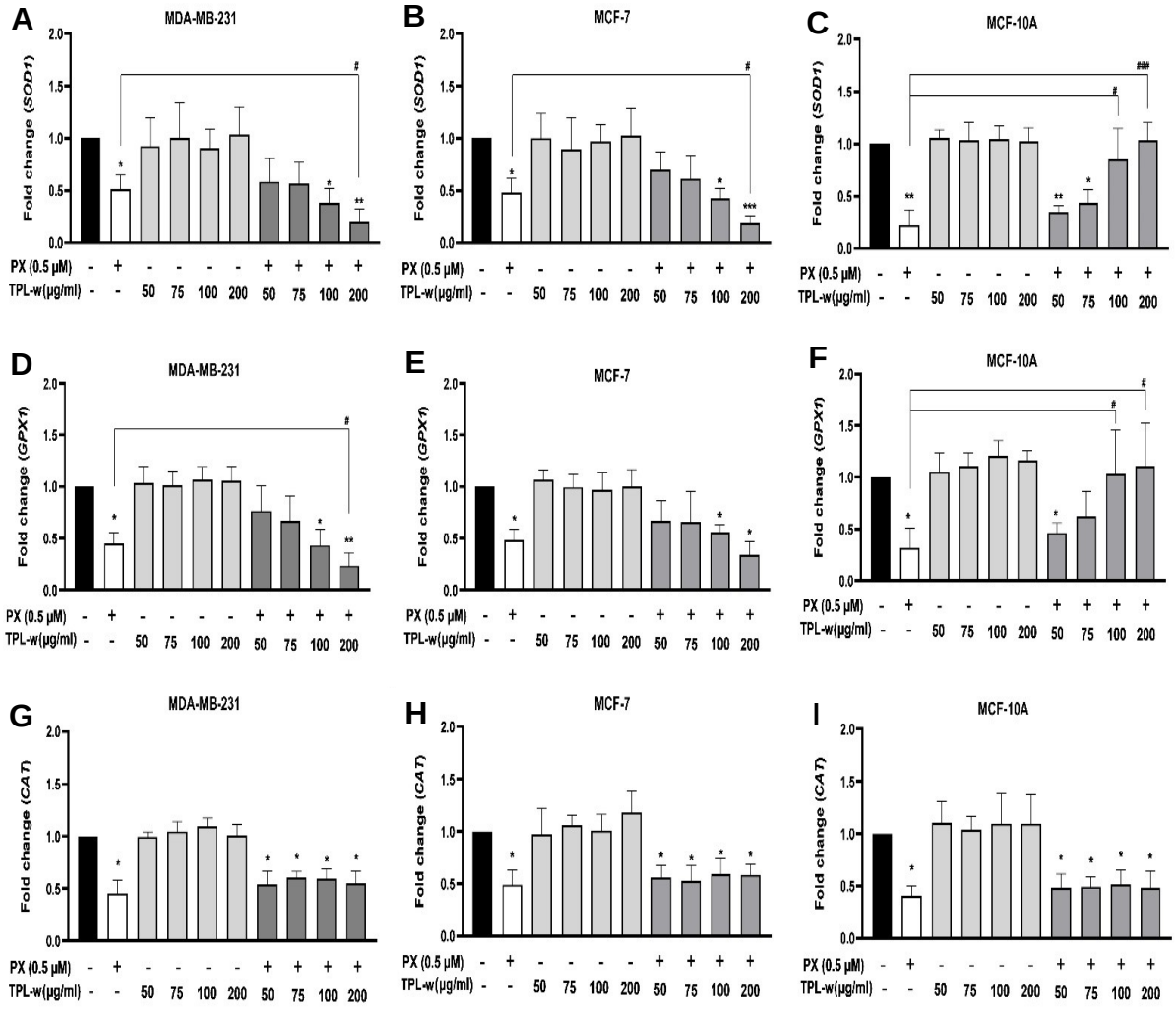


**Figure 7**. Effects of TPL-w combined with low-dose PX on *SOD1* (**A–C**), *GPX1* (**D–F**), and *CAT* (**G–I**) mRNA expression in MDA-MB-231 (**A, D, G**), MCF-7 (**B, E, H**), and MCF-10A (**C, F, I**) cells. Expression levels were normalized to β-actin. Data are presented as mean ± SEM from three independent experiments performed in triplicate. Statistical significance was defined as $^{*}P < 0.05$; $^{**}P < 0.01$; $^{***}P < 0.001$ compared to untreated cells, and $^{\#}P < 0.05$; $^{\#\#}P < 0.01$; $^{\#\#\#}P < 0.001$ compared to PX-treated cells.

$P$ = 0.007) cells (**Figure 7A-C**, **8A-C**). The combination of PX with 200 µg/mL of TPL-w further suppressed *SOD1* expression in the MDA-MB-231 (2.7-fold, $P = 0.042$) and MCF-7 (2.6-fold, $P = 0.020$) cells (**Figure 7A-B**). A similar trend was observed for 100 and 200 µg/mL of TPL-a, resulting in a 3.6–3.9-fold reduction in the MDA-MB-231 cells ($P = 0.035$ and $P = 0.020$) and a 2.0–3.4-fold decrease in the MCF-7 cells ($P = 0.045$ and $P = 0.022$) (**Figure 8A-B**). Interestingly, in the MCF-10A cells, treatment with 100 and 200 µg/mL of TPL significantly increased *SOD1* expression compared with that of PX alone, with a 3.6–4.1-fold increase ($P = 0.028$ and $P < 0.001$) in the TPL-w group (**Figure 7C**) and a 4.5–4.9-fold increase ($P = 0.008$ and $P < 0.001$) in the TPL-a group (**Figure 8C**).

PX treatment also downregulated *GPX1* expression in the MDA-MB-231 (2.2-fold, $P = 0.018$), MCF-7 (2.1-fold, $P = 0.034$), and MCF-10A (3.1-fold, $P$ = 0.011) cells. The combination treatment further reduced *GPX1* expression in the MDA-MB-231 cells when cotreated with TPL-w (1.9-fold, $P$ = 0.038)

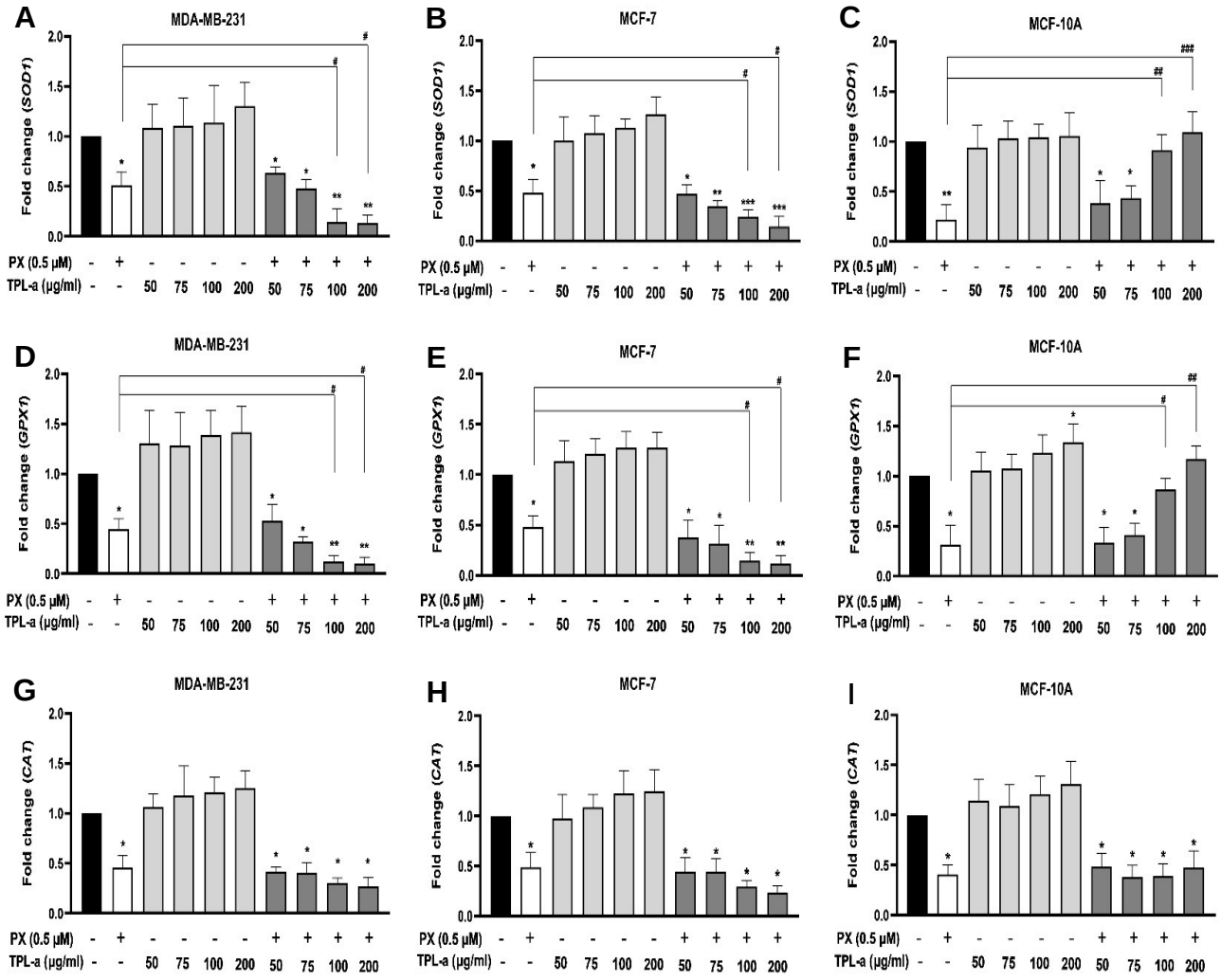


**Figure 8**. Effects of TPL-a combined with low-dose PX on *SOD1* (**A–C**), *GPX1* (**D–F**), and *CAT* (**G–I**) mRNA expression in MDA-MB-231 (**A, D, G**), MCF-7 (**B, E, H**), and MCF-10A (**C, F, I**) cells. Expression levels were normalized to β-actin. Data are presented as mean ± SEM from three independent experiments performed in triplicate. Statistical significance was defined as $^{*}P < 0.05$; $^{**}P < 0.01$; $^{***}P < 0.001$ compared to untreated cells, and $^{\#}P < 0.05$; $^{\#\#}P < 0.01$; $^{\#\#\#}P < 0.001$ compared to PX-treated cells.

(**Figure 7D**) and with 100 and 200 μg/mL of TPL-a (3.0–3.3-fold, $P = 0.015$ and $P = 0.011$) (**Figure 8D**). Similarly, in the MCF-7 cells, 100 and 200 μg/mL of TPL-a decreased *GPX1* expression by 3.3–4.2-fold ($P = 0.025$ and $P = 0.019$) (**Figure 8E**). In contrast, *GPX1* expression in the MCF-10A cells increased 3.0–3.5-fold following treatment with 100 and 200 μg/mL of TPL-w ($P = 0.028$ and $P = 0.012$) (**Figure 7F**) and 2.7–3.7-fold following treatment with 100 and 200 μg/mL of TPL-a ($P = 0.042$ and $P = 0.008$) (**Figure 8F**).

PX treatment alone significantly reduced *CAT* expression in the MDA-MB-231 (2.2-fold, $P = 0.046$), MCF-7 (2.0-fold, $P = 0.043$), and MCF-10A (2.5-fold, $P = 0.031$) cells. However, the combination of PX and TPL extracts did not induce any significant changes in *CAT* expression across all cell lines (**Figure 7G-I, 8G-I**).

## Discussion

Numerous studies have highlighted TPL's potent antioxidant properties, primarily attributed to its polyphenol content. [12] These compounds act as natural antioxidants by neutralizing free radicals and preventing cellular damage. [23] Consistent with previous research, our study evaluated the antioxidant activity of TPL-w and TPL-a, with the latter demonstrating superior free radical scavenging ability. HPLC analysis identified gallic acid as the primary compound, which aligns with the findings of previous studies. [24] Moreover, we observed a higher total phenolic content than flavonoid content in both extracts. The superior antioxidant activity and phenolic content in the ethanolic extract likely resulted from ethanol's greater efficiency in extracting phenolic compounds. [25] Previous studies identified 18 compounds in TPL, with gallic acid comprising approximately 30% of the extract, in addition to other polyphenols. [24] However, variations in phytochemical composition due to plant origin and geography should be considered. These findings further support the use of ethanol as a superior solvent for extracting bioactive TPL compounds.

Redox homeostasis is critical for cell survival. Although normal cells maintain low levels of ROS, cancer cells exhibit elevated levels of ROS due to their heightened metabolic activity, promoting tumor progression while triggering antioxidant defenses. [26, 27] Our previous findings confirmed that TNBC cells, particularly MDA-MB-231, exhibit higher basal levels of ROS than normal breast cells. [7] As TNBC cells rely on ROS for survival, antioxidant treatment reduces proliferation and induces cell death, thus highlighting ROS as a therapeutic target. [6]

Natural antioxidants, such as gallic acid and TPL, are gaining attention in cancer therapy for their ability to induce apoptosis and cell cycle arrest while sparing normal cells. [28] Consistent with previous studies, our findings demonstrated the anticancer activity of TPL extracts in MDA-MB-231 and MCF-7 cells, with higher $IC_{50}$ values in normal cells, thereby emphasizing TPL's safety profile. [29]

Chemotherapy is effective, but its use is limited by toxicity to normal tissues. We found that even low-dose PX treatment reduced MCF-10A cell survival. Notably, TPL extract enhanced PX-induced cytotoxicity in breast cancer cells while protecting normal cells. CI values < 1 confirmed synergy in cancer cells, while an antagonistic effect (CI > 1) was observed in MCF-10A cells, which suggests that TPL enhances chemotherapy efficacy while mitigating its toxicity against normal cells. Although the role of polyphenols in chemotherapy-induced antagonism remains understudied [30], our findings suggest that TPL's antioxidant properties contribute to reducing the ROS-mediated toxicity in normal cells.

Apoptosis plays an essential role in cancer therapy. We assessed the expression of BAX (pro-apoptotic) and BCL2 (anti-apoptotic) to evaluate TPL's apoptotic effects. Low-dose PX treatment increased the *BAX/BCL2* ratio, whereas PX and TPL cotreatment further elevated this ratio in breast cancer cells, thereby indicating enhanced apoptosis. Conversely, TPL reduced the *BAX/BCL2* ratio in MCF-10A cells, thus highlighting its protective role. Previously, lauryl gallate, a gallic acid derivative, enhanced chemotherapy efficacy while minimizing side effects [31], which aligns with our findings.

Chemotherapy-induced oxidative stress plays a substantial role in its cytotoxic effects, with PX increasing the ROS levels and causing mitochondrial dysfunction. [32] Our study confirmed that low-dose PX elevated the ROS levels in cancer and normal cells. However, TPL, which is known for its prooxidant activity in breast cancer cells [14], further increased the ROS levels in breast cancer cells [33] while reducing the ROS levels in normal cells. Similar protective effects were previously observed in normal murine spleen and liver cells, where TPL mitigated chemotherapy-induced ROS production. [29] Notably, combination treatment with low-dose PX with TPL significantly decreased intracellular ROS in MCF-10A cells, while high-dose TPL further reduced the ROS to near-baseline levels.

These findings highlight the dual role of TPL in promoting oxidative stress in cancer cells while protecting normal tissues. This suggests that polyphenols exploit cancer cells' redox imbalance, enhancing their vulnerability while safeguarding healthy cells. However, the precise mechanism by which polyphenols specifically induce ROS accumulation in breast cancer cells remains unclear and warrants further investigation.

Cellular antioxidant enzymes, including SOD, CAT, and GPX, maintain the redox balance by neutralizing excess ROS. SOD converts superoxide radicals into hydrogen peroxide, which is further broken down by CAT and GPX to prevent cellular damage. [34]

Chemotherapy disrupts this balance by increasing ROS accumulation and reducing antioxidant enzyme levels. Consistent with previous studies, our results showed decreased expression of *SOD1*, *CAT*, and *GPX1* following low-dose PX treatment. Moreover, PX and TPL cotreatment further decreased the expression of *SOD1* and *GPX1* in breast cancer cells while upregulating these enzymes in normal cells, thereby mitigating oxidative stress. High-dose TPL combined with PX significantly restored *SOD1* and *GPX1* expression, rescued redox homeostasis in MCF-10A cells, reduced ROS levels, and minimized cell death. These findings highlight TPL's potential in mitigating chemotoxicity through the upregulation of antioxidant genes.

Although CAT is a primary antioxidant enzyme, our study found no significant changes in its expression following TPL treatment. This result aligns with that of previous reports, which showed that low CAT levels in breast cancer cells are due to reduced peroxisome activity. [35-37] The higher affinity of GPX for hydrogen peroxide may also have contributed to this observation. Further research is required to clarify the regulation of CAT in breast cancer cells.

Overall, our findings indicate that TPL enhances PX-induced cytotoxicity in breast cancer cells while protecting normal breast epithelial cells. This dual effect likely stems from differential ROS levels and oxidative stress responses. TPL promotes cancer cell apoptosis by increasing ROS accumulation, downregulating the expression of *SOD1* and *GPX1*, and elevating the *BAX/BCL2* ratio. In contrast, it preserves the redox balance in normal cells by upregulating antioxidant enzymes and reducing apoptosis. These results align with previous studies demonstrating selective chemotherapy toxicity in cancer versus normal cells. [38] In addition, combining chemotherapeutic agents with redox-modulating compounds, such as TPL, has been proposed to enhance the treatment efficacy, reduce the required drug doses, and minimize the adverse effects **(Figure 9).** [39]

Although our study provides important insights into TPL's dual actions, it is limited by the lack of mechanistic investigations into the apoptosis pathways. We assessed only the expression of key apoptotic and antioxidant genes without examining upstream regulators such as ROS-mediated signaling, Akt, endoplasmic reticulum stress, or mitochondrial dysfunction. These aspects merit further investigation to better understand the pathways through which TPL modulates cell survival and death. Moreover, future *in vivo* studies are required to confirm the therapeutic potential of TPL. Nevertheless, our results support the potential of TPL as a promising adjuvant to enhance chemotherapy efficacy while minimizing toxicity to normal tissues.

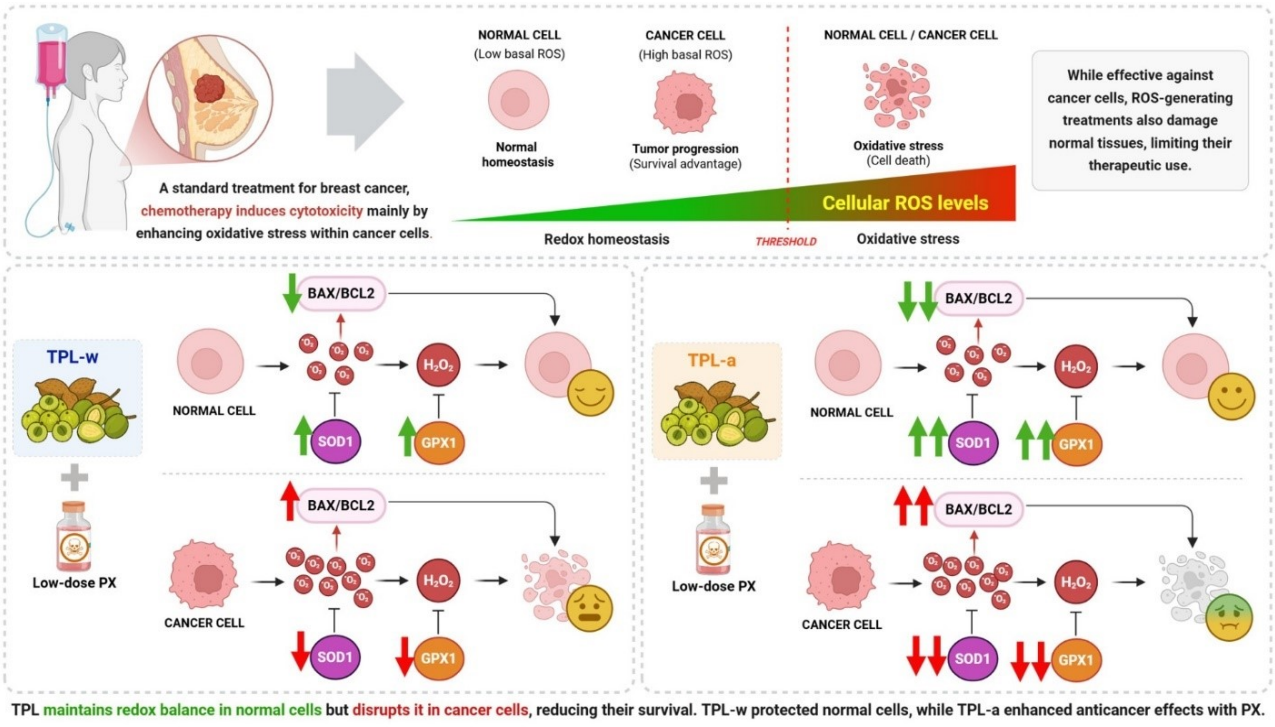


**Figure 9.** Dual role of TPL extracts in breast cancer therapy.

## Conclusion

This study demonstrates that TPL extracts enhance chemotherapy-induced cytotoxicity in breast cancer cells while protecting normal cells. The ethanolic extract, rich in gallic acid, exhibits superior antioxidant and prooxidant activities and promotes ROS accumulation and apoptosis in cancer cells while preserving the redox balance in normal cells. These findings highlight TPL's potential as a safe and effective adjunct to chemotherapy, and further *in vivo* studies are warranted to elucidate its precise molecular mechanisms and therapeutic applications.

### Acknowledgements

This work was supported by the 90th Anniversary of Chulalongkorn University Fund (Ratchadaphiseksomphot Endowment Fund).

### Conflict of interest statement

The authors declare that they have no conflicts of interest.

### Data sharing statement.

All data generated or analyzed in this study are included within this published article. Additional details are available for non-commercial purposes from the corresponding author upon reasonable request.

## References

1. Giaquinto AN, Sung H, Newman LA, Freedman RA, Smith RA, Star J, et al. Breast cancer statistics 2024. CA Cancer J Clin 2024;74:477–95.
2. Perou CM, Sørlie T, Eisen MB, van de Rijn M, Jeffrey SS, Rees CA, et al. Molecular portraits of human breast tumours. Nature 2000;406:747–52.
3. Pham-Huy LA, He H, Pham-Huy C. Free radicals, antioxidants in disease and health. Int J Biomed Sci 2008;4:89–96.
4. Yang HT, Villani RM, Wang HL, Simpson MJ, Roberts MS, Tang M, et al. The role of cellular reactive oxygen species in cancer chemotherapy. J Exp Clin Canc Res 2018;37:266.
5. Weinberg F, Hamanaka R, Wheaton WW, Weinberg S, Joseph J, Lopez M, et al. Mitochondrial metabolism and ROS generation are essential for Kras-mediated tumorigenicity. Proc Natl Acad Sci U S A 2010;107:8788–93.
6. Sarmiento-Salinas FL, Delgado-Magallón A, Montes-Alvarado JB, Ramirez-Ramírez D, Flores-Alonso JC, Cortes-Hernandez P, et al. Breast cancer subtypes present a differential production of reactive oxygen species (ROS) and susceptibility to antioxidant treatment. Front Oncol 2019;9:480.
7. Charucharana S, Cheepsunthorn P, Cheepsunthorn CL. Antioxidant and chemotherapeutic synergy: Triphala enhances doxorubicin cytotoxicity in breast cancer cells and reduces toxicity in non-tumorigenic cells. Chula Med J 2025;69:95–108.
8. Xiao H, Verdier-Pinard P, Fernandez-Fuentes N, Burd B, Angeletti R, Fiser A, et al. Insights into the mechanism of microtubule stabilization by Taxol. Proc Natl Acad Sci U S A 2006;103:10166–73.
9. Yang HT, Villani RM, Wang HL, Simpson MJ, Roberts MS, Tang M, et al. The role of cellular reactive oxygen species in cancer chemotherapy. J Exp Clin Cancer Res 2018;37:266.
10. Zhang Y, Tang Y, Tang X, Wang Y, Zhang Z, Yang H. Paclitaxel induces the apoptosis of prostate cancer cells via ROS-mediated HIF-1alpha expression. Molecules 2022;27:7183.
11. Wargo JA, Reuben A, Cooper ZA, Oh KS, Sullivan RJ. Immune effects of chemotherapy, radiation, and targeted therapy and opportunities for combination with immunotherapy. Semin Oncol 2015;42:601–16.
12. Priyadrsini I, Mohan H, Naik G. An ayurvedic remedy - triphala as antioxidant drug. Antioxidants, Nutrients & Health. Free Radical Biol Med 2003;35 (Suppl):S43.
13. Cheriyamundath S, Mahaddalkar T, Save SN, Choudhary S, Hosur RV, Lopus M. Aqueous extract of Triphala inhibits cancer cell proliferation through perturbation of microtubule assembly dynamics. Biomed Pharmacother 2018;98:76–81.
14. Sandhya T, Mishra KP. Cytotoxic response of breast cancer cell lines, MCF 7 and T 47 D to triphala and its modification by antioxidants. Cancer Lett 2006;238: 304–13.
15. Kaur S, Michael H, Arora S, Härkönen PL, Kumar S. The in vitro cytotoxic and apoptotic activity of Triphala - an Indian herbal drug. J Ethnopharmacol 2005;97: 15–20.
16. Jagetia GC, Malagi KJ, Baliga MS, Venkatesh P, Veruva RR. Triphala, an ayurvedic Rasayana drug, protects mice against radiation-induced lethality by free-radical scavenging. J Altern Complement Med 2004;10:971–8.
17. Naik GH, Priyadarsini KI, Bhagirathi RG, Mishra B, Mishra KP, Banavalikar MM, et al. In vitro antioxidant studies and free radical reactions of triphala, an ayurvedic formulation and its constituents. Phytother Res 2005;19:582–6.
18. Zhu J, Yi X, Zhang J, Chen S, Wu Y. Chemical profiling and antioxidant evaluation of Yangxinshi Tablet by HPLC-ESI-Q-TOF-MS/MS combined with DPPH assay. J Chromatogr B Analyt Technol Biomed Life Sci 2017;1060:262–71.

19. Meena AK, Narasimhaji CV, Velvizhi D, Singh A, Rekha P, Kumar V, et al. Determination of gallic acid in ayurvedic polyherbal formulation Triphala churna and its ingredients by HPLC and HPTLC. Res J Pharm Technol 2018;11:3243–9.
20. Ainsworth EA, Gillespie KM. Estimation of total phenolic content and other oxidation substrates in plant tissues using Folin-Ciocalteu reagent. Nat Protoc 2007;2:875–7.
21. Fattahi S, Zabihi E, Abedian Z, Pourbagher R, Motevalizadeh Ardekani A, Mostafazadeh A, et al. Total phenolic and flavonoid contents of aqueous extract of stinging nettle and in vitro antiproliferative effect on Hela and BT-474 cell lines. Int J Mol Cell Med 2014;3: 102–7.
22. Chou TC. Theoretical basis, experimental design, and computerized simulation of synergism and antagonism in drug combination studies. Pharmacol Rev 2006;58: 621–81.
23. Grace SC. Phenolics as antioxidants. In: Smirnoff N, editor. Antioxidants and reactive oxygen species in plants. Oxford, UK: Blackwell Publishing; 2005. p. 141 –68.
24. Prasad S, Srivastava SK. Oxidative stress and cancer: chemopreventive and therapeutic role of Triphala. Antioxidants (Basel) 2020;9:72.
25. Wang L, Weller CL. Recent advances in extraction of nutraceuticals from plants. Trends Food Sci Technol 2006;17:300–12.
26. Panieri E, Santoro MM. ROS homeostasis and metabolism: a dangerous liason in cancer cells. Cell Death Dis 2016;7:e2253.
27. Gorrini C, Harris IS, Mak TW. Modulation of oxidative stress as an anticancer strategy. Nat Rev Drug Discov 2013;12:931–47.
28. Abotaleb M, Liskova A, Kubatka P, Busselberg D. Therapeutic potential of plant phenolic acids in the treatment of cancer. Biomolecules 2020;10:221.
29. Sandhya T, Lathika KM, Pandey BN, Mishra KP. Potential of traditional ayurvedic formulation, Triphala, as a novel anticancer drug. Cancer Lett 2006;231: 206–14.
30. Èipák L, Novotný L, Èipáková I, Rauko P. Differential modulation of cisplatin and doxorubicin efficacies in leukemia cells by flavonoids. Nutr Res 2003;23: 1045–57.
31. Ghatreh Samani K, Farrokhi E, Tabatabaee A, Jalilian N, Jafari M. Synergistic effects of lauryl gallate and tamoxifen on human breast cancer cell. Iran J Public Health 2020;49:1324–9.
32. Alexandre J, Batteux F, Nicco C, Chéreau C, Laurent A, Guillevin L, et al. Accumulation of hydrogen peroxide is an early and crucial step for paclitaxel-induced cancer cell death both in vitro and in vivo. Int J Cancer 2006;119:41–8.
33. Moghtaderi H, Sepehri H, Delphi L, Attari F. Gallic acid and curcumin induce cytotoxicity and apoptosis in human breast cancer cell MDA-MB-231. Bioimpacts 2018;8:185–94.
34. Ighodaro OM, Akinloye OA. First line defence antioxidants-superoxide dismutase (SOD), catalase (CAT) and glutathione peroxidase (GPX): Their fundamental role in the entire antioxidant defence grid. Alex J Med 2018;54:287–93.
35. Glorieux C, Zamocky M, Sandoval JM, Verrax J, Calderon PB. Regulation of catalase expression in healthy and cancerous cells. Free Radic Biol Med 2015;87:84–97.
36. Walton PA, Brees C, Lismont C, Apanasets O, Fransen M. The peroxisomal import receptor PEX5 functions as a stress sensor, retaining catalase in the cytosol in times of oxidative stress. Biochim Biophys Acta Mol Cell Res 2017;1864:1833–43.
37. Marklund SL, Westman NG, Lundgren E, Roos G. Copper- and zinc-containing superoxide dismutase, manganese-containing superoxide dismutase, catalase, and glutathione peroxidase in normal and neoplastic human cell lines and normal human tissues. Cancer Res 1982;42: 1955–61.
38. Wang S, Konorev EA, Kotamraju S, Joseph J, Kalivendi S, Kalyanaraman B. Doxorubicin induces apoptosis in normal and tumor cells via distinctly different mechanisms. intermediacy of H(2)O(2)- and p53-dependent pathways. J Biol Chem 2004;279:25535–43.
39. Vijay K, Sowmya PR, Arathi BP, Shilpa S, Shwetha HJ, Raju M, et al. Low-dose doxorubicin with carotenoids selectively alters redox status and upregulates oxidative stress-mediated apoptosis in breast cancer cells. Food Chem Toxicol 2018;118:675–90.